IL NUOVO CIMENTO Vol. 112 A, N. 7 Luglio 1999

The effect of level density and reaction mechanisms on the reaction cross-section calculations at intermediate energies

V. P. Lunev([1]), Yu. N. Shubin([1]), C. Grandi([2]), B. Poli([2]) and A. Ventura([3])([4])

([1]) *Institute of Physics and Power Engineering - 249020 Obninsk, Russia*
([2]) *Dipartimento di Fisica dell'Università di Bologna Viale Berti Pichat 6/2, 40127 Bologna, Italy*
([3]) *ENEA, Centro Dati Nucleari - Via Martiri di Monte Sole 4, 40129 Bologna, Italy*
([4]) *INFN, Sezione di Bologna - Viale Berti Pichat 6/2, 40127 Bologna, Italy*

(ricevuto l'8 Marzo 1999; approvato il 24 Maggio 1999)

Summary. — Two versions of the pre-equilibrium ALICE code (HMS-ALICE and ALICE-IPPE) were used to investigate the effect of various models for level density and cluster emission mechanisms on the description of reaction cross-sections with multiple-particle emission induced by protons of energy up to 200 MeV in a mass region from Mn to Bi. Comparison with experimental data shows that the generalised superfluid model for level density is preferable for nuclei far from the beta stability line. For the reactions where composite charged particles can be produced, the account of both pick-up and knock-out mechanisms can be crucial for the consistent description of excitation functions in the energy region 30–80 MeV where the pre-equilibrium cluster emission and emission of several uncorrelated nucleons compete.

PACS 24.10 – Nuclear reaction models and methods.
PACS 24.50 – Direct reactions.
PACS 24.60.Gv – Statistical multistep direct reactions.
PACS 25.40 – Nucleon-induced reactions.

1. – Introduction

To develop the main concepts of accelerator-driven power systems and the corresponding nuclear waste management, it is necessary to know nuclear data on spectra and reaction cross-sections for structural materials, actinides and the most important fission products in a very broad energy range. In practice, the interval from thermal energies to some thousands MeV should be covered [1,2]. The status of available nuclear data differs considerably for the energy regions below and above 20 MeV. As known, huge

efforts have been made to create libraries of evaluated neutron data, such as ENDF/B, JENDL, BROND, etc., for the low-energy region. In spite of some differences among the evaluations, the majority of data are reasonable enough and their accuracy satisfies the requirements of major current applications. For the energies higher than 20 MeV the situation is different, data are rather scarce and are not systematised yet.

Lack of experimental data should be compensated by the development of reliable models and computational methods. The codes based on intranuclear cascade model combined with evaporation model have been successfully applied for incident nucleon energies above several hundred MeV [3-8]. However, at lower energies, nuclear structure effects can be so prominent that their description requires more detailed consideration of competitive reaction mechanisms. Therefore, it has been proposed that the energy region from 20 to 200 MeV requires special investigation [1, 2].

We have carried out calculations and comparison with experimental data in the energy region up to 200 MeV using two versions of the pre-equilibrium model (PE) ALICE code (HMS-ALICE [9, 10] and ALICE-IPPE [11]) for nuclei in the mass region from Mn to Bi. Different approaches to the description of level densities of excited nuclei and various mechanisms of emission of composite charged particles (clusters) were used in the calculations. The analysis performed in this work has shown that the choice of level density model considerably affects the computational results: in particular, the more comprehensive generalised superfluid model [11] gives better description of the reaction cross-sections in the energy region considered. For reactions with multiple-particle emission, when composite charged particles can be produced, proper account of reaction mechanisms can be crucial for the consistent description of excitation functions in the energy region 30–80 MeV, where pre-equilibrium cluster emission and emission of several uncorrelated particles compete.

In sect. **2** we briefly summarise the physics in the HMS-ALICE code, largely with reference to published works. In sect. **3** we outline the main improvements in the ALICE-IPPE code used in the calculations: the generalised superfluid model for level density and the model for the pre-equilibrium emission of clusters that takes into account both the knock-out and pick-up processes. The results of calculations using different codes, comparison with experimental data and discussion are presented in sect. **4**.

2. – The HMS-ALICE Code

The HMS-ALICE approach (Hybrid model Monte Carlo Simulation) [9] uses simple "exciton" energy partition algorithms to follow the fast cascade, until nucleon energies are so close to the binding energy that they become part of the equilibrated ensemble. The fast cascade aspects of the code are fixed *a priori*, whereas there are a multitude of parameters which might be adjusted in the fission-evaporation phase. For the fission rate, the code uses the liquid-drop-model barriers due to Mebel [8], and a ratio of fission to evaporation level density parameters of 1.02. The HMS-ALICE code has several options which may be used for evaporation level densities. The default option is the Fermi gas model, but shell-corrected level densities due to Kataria and Ramamurthy, or Ignatyuk, or Gilbert-Cameron may also be selected.

In the present work, we have used HMS-ALICE with a standard set-up originally suggested by the author, M. Blann, for a comparison with the intranuclear cascade-evaporation-fission (CEF) code [7,8] focused on activation yields in proton-induced reactions on fissile and non-fissile isotopes in the energy range from 50 MeV to 1.8 GeV [12]. Both CEF and HMS-ALICE turned out to be generally successful in reproducing the

experimental yields and yield patterns.

3. – The ALICE-IPPE code

Here, we outline the two main changes in the level density model and mechanisms of pre-equilibrium emission of light composite particles (clusters) incorporated into the ALICE-IPPE version of the code.

3˙1. *Level density.* – Nuclear level densities play a significant role in the description of reaction cross-sections within the framework of statistical nuclear theory. To calculate it, use is made of various versions of the Fermi-gas model, which are attractive because of their simplicity [13]. However, the analysis performed on the basis of the microscopic approach to nuclear structure has shown that the Fermi-gas model does not take into account many fundamental properties of excited nuclei, connected with the shell structure of the single-particle spectrum, the pairing correlations of superconductive type and the coherent collective excitations of nuclei in a consistent way. The generalised superfluid model for level density developed in IPPE, on the one hand, takes into account the basic theoretical concepts and results and is, on the other hand, relatively simple and convenient for practical use [13-18].

3˙2. *Generalised superfluid model.* – In the generalised superfluid model, nuclear states can be subdivided [13-18] into intrinsic (quasiparticle) excitations and collective excitations. On the simplifying assumption of decoupling of quasiparticle and collective degrees of freedom, the level density can be written as follows:

$$\omega(U') = \rho_{\mathrm{qp}}(U') \cdot K_{\mathrm{vib}}(U') \cdot K_{\mathrm{rot}}(U'), \tag{1}$$

where $\rho_{\mathrm{qp}}(U')$ is the density of quasiparticle (non-collective) excited states, $K_{\mathrm{vib}}(U')$ and $K_{\mathrm{rot}}(U')$ are the coefficients of the enhancement of the level density due to the vibrational and rotational states, respectively, at the effective excitation energy U'.

The energy dependence of the quasiparticle state density is calculated on the basis of the equations of the superfluid model [13-19]. The correlation function for the ground states is chosen equal to $\Delta_0 = 12.0/A^{1/2}$ MeV. Such a choice is consistent, on the average, with nuclear mass systematics [20] and with results of the analysis of the densities of neutron resonances for heavy nuclei [18]. The critical temperature of the phase transitions from the superfluid state to the normal one, the critical energy of the phase transition, the condensation energy and the effective excitation energy are connected with the correlation function Δ_0 by the following equations [19]:

$$\begin{aligned} t_{\mathrm{cr}} &= 0.567\Delta_0, \\ E_{\mathrm{cr}} &= 0.472\, a_{\mathrm{cr}}{\Delta_0}^2 - n\Delta_0, \\ E_{\mathrm{con}} &= 0.152\, a_{\mathrm{cr}}{\Delta_0}^2 - n\Delta_0, \\ U' &= U + n\Delta_0 + \delta_{\mathrm{shift}}, \end{aligned} \tag{2}$$

where $a_{\mathrm{cr}} = a(U_{\mathrm{cr}})$ is the level density parameter (in MeV^{-1}) computed at the critical excitation energy, $U' = U_{\mathrm{cr}}$, and $n = 0$, 1 and 2 for even-even, odd-mass and odd-odd nuclei, respectively. The empirical value of the energy shift, δ_{shift}, was determined on

the basis of a consistent description of densities of low-lying discrete states and densities of neutron resonances. Shell effects were included in the phenomenological energy dependence of the level density parameter, $a(U, A)$:

$$a(U,Z,A) = \begin{cases} \tilde{a}(A) \cdot \left(1 + \delta W(Z,A) \cdot \frac{\varphi(U' - E_{\rm cond})}{U' - E_{\rm cond}}\right), & \text{for } U' > U_{\rm cr}, \\ a(U_{\rm cr}, Z, A), & \text{for } U' < U_{\rm cr}. \end{cases} \tag{3}$$

Here, the asymptotic value of the level density parameter, in MeV^{-1}, at high excitation energy was chosen to be

$$\tilde{a}(A) = 0.073A + 0.115A^{2/3}; \tag{4}$$

$\delta W(Z, A)$ is the shell correction to the binding energy of nuclei, determined either from the experimental masses or by means of the Myers-Swiatecki formula [20, 21], $\varphi(U) = 1 - \exp[-\gamma U]$ is a dimensionless function, which gives the energy dependence of the level density parameter at low excitation energy. The value $\gamma = 0.4/A^{1/3}\,\mathrm{MeV}^{-1}$ was determined from the analysis of neutron resonance densities [13-19].

The vibrational enhancement of level densities can be calculated as follows:

$$K_{\rm vib} = \exp\left[\delta S - \left(\frac{\delta U}{t}\right)\right], \tag{5}$$

where the variations of entropy, δS, and excitation energy, δU, due to the collective excitation modes, can be found from the equations for the Bose gas

$$\begin{aligned} \delta S &= \sum_{i=1}^{\infty} (2\lambda_i + 1)\big\{(1+n_i)\ln(1+n_i) - n_i \ln(n_i)\big\}, \\ \delta U &= \sum_{i=1}^{\infty} (2\lambda_i + 1)\omega_i n_i, \end{aligned} \tag{6}$$

where ω_i and λ_i are the energy and multipolarity of collective phonons of the i-th type, respectively, and n_i is the phonon occupation number at finite temperature. The damping of the collective enhancement of level density with increasing temperature was taken into account according to the following temperature dependence of the phonon numbers:

$$n_i = \frac{\exp[-\gamma_i/(2\omega_i)]}{\exp[\omega_i/t] - 1}. \tag{7}$$

The value of the γ_i parameter, in MeV, was found from the consistent description of low-lying levels and neutron resonance data:

$$\gamma_i = 0.0075A^{1/3}(\omega_i^2 + 4\pi^2 t^2). \tag{8}$$

In the vibrational enhancement factor, the most significant contributions to positive and negative parity states are expected from quadrupole and octupole modes, respectively.

The position of the lowest multipole excitations for all nuclei, except ^{208}Pb, was defined according to phenomenological formulas, which describe the experimental data rather well:

$$\omega_2 = 30A^{-1/3}, \qquad \omega_3 = 50A^{-1/3}. \tag{9}$$

Here, both energies are expressed in MeV.

In the case of ^{208}Pb, the position of the lowest 2^+ excitation was set to 4.1 MeV from the experiment.

For spherical nuclei, only the vibrational enhancement factor, $K_{\mathrm{vib}}(U')$, was taken into account. For deformed nuclei, the rotational enhancement factor, $K_{\mathrm{rot}}(U')$, was included, too, according to the equation [19]

$$K_{\mathrm{rot}}(U) = \sigma_{\perp}^2 g(U) = \sigma^2(1+\beta/3)g(U). \tag{10}$$

Here σ is the spin cut-off parameter, and $g(U)$ is an empirical function, which takes into account the damping of the rotational modes with increasing temperature, in the form proposed by Hansen and Jensen [22]:

$$g(U) = \left\{1 + \exp\left[\frac{U-U_r}{d_r}\right]\right\}^{-1}, \tag{11}$$

where the parameters U_r and d_r, in MeV, are the following functions of the nuclear quadrupole deformation, β:

$$U_r = 120A^{1/3}\beta^2; \qquad d_r = 1400A^{-2/3}\beta^2. \tag{12}$$

The β parameter is defined from the nuclear mass formula of Myers and Swiatecki [20, 21].

3·3. *Pre-equilibrium cluster emission*

3·3.1. Pre-equilibrium deuteron emission. The approach to the computation of energy spectra of deuterons emitted in non-elastic interactions is briefly discussed below. Deuteron differential cross-sections calculated in the frame of the coalescence pick-up model [23, 24] without inclusion of direct processes show considerable disagreement with experimental data [11], because the direct mechanism of deuteron production always gives an important contribution to the energy spectrum, according to ref. [25].

Direct processes in deuteron emission can be taken into account using a phenomenological approach based on the hybrid exciton model. To this end, we consider nucleon pick-up and deuteron emission from the initial one particle-zero hole configuration $(1p0h)$ [26,27]. The energy spectrum in pre-equilibrium deuteron emission can be written in the following form:

$$\frac{\mathrm{d}\sigma^{\mathrm{pre}}}{\mathrm{d}\varepsilon_{\mathrm{d}}} = \sigma_{\mathrm{non}}\left\{\frac{\omega^*(E-Q_{\mathrm{d}}-\varepsilon_{\mathrm{d}})}{\omega(1p,0h,E)}\cdot\frac{\lambda_{\mathrm{c}}^{\mathrm{d}}}{\lambda_{\mathrm{c}}^{\mathrm{d}}+\lambda_{+}^{\mathrm{d}}}\cdot g_{\mathrm{d}} + \right. \tag{13}$$

$$\left. + \sum_{n=3}\sum_{l+m=2} F_{l,m}(\varepsilon_{\mathrm{d}})\cdot\frac{\omega(p-l,h,E-Q_{\mathrm{d}}-\varepsilon_{\mathrm{d}})}{\omega(p,h,E)}\cdot\frac{\lambda_{\mathrm{c}}^{\mathrm{d}}}{\lambda_{\mathrm{c}}^{\mathrm{d}}+\lambda_{+}^{\mathrm{d}}}\cdot g_{\mathrm{d}}D_{\mathrm{n}}\right\},$$

where $\sigma_{\rm non}$ is the non-elastic interaction cross-section of the incident nucleon with the target nucleus, the first term in braces of eq. (13) corresponds to the direct deuteron emission from the initial configuration and the second term to the formation of deuterons by pick-up in the nuclear surface region, according to ref. [23]; $\omega^*(U)$ is the state density at excitation energy U of the residual nucleus after deuteron emission, $g_{\rm d}$ is the single-particle level density for deuterons, $\omega(p,h,E)$ is the density of states with fixed exciton number, $n = p + h$, at excitation energy E, p being the number of particles and h the number of holes, $Q_{\rm d}$ is the deuteron binding energy and $\varepsilon_{\rm d}$ its kinetic energy in the continuum, $\lambda_{\rm c}^{\rm d}(\varepsilon_{\rm d})$ is the deuteron emission rate in the continuum, while $\lambda_{+}^{\rm d}$ is the deuteron intra-nuclear transition rate. In the second term in braces on the right-hand side of eq. (13), F_{lm} is a deuteron formation factor by pick-up in the nuclear surface region of l particles and m holes, defined in refs. [23, 24], and D_n is a depletion factor of the n-exciton state, which measures the loss of flux by deuteron emission.

Coming back to the first term in braces on the right-hand side of eq. (13), after emission of a deuteron formed by nucleon pick-up from a (p,h) configuration the final state of the nucleus is $(p-1, h+1)$. Therefore, the density of final states, $\omega^*(U)$, can be written in the form

$$\omega^*(U) = \frac{\omega(0p, 1h, U)\gamma}{g_{\rm d}}, \tag{14}$$

where γ is a value characterizing the deuteron formation.

The comparison of the deuteron emission spectra calculated with eqs. (13) and (14) and the measured spectra made it possible to establish that the γ parameter is weakly dependent on the atomic mass number of the target nucleus, so that it can be taken to be constant with good accuracy.

3˙3.2. Pre-equilibrium α-emission. The energy spectrum of α-particles emitted in an intermediate-energy reaction can be represented as a sum of three components, corresponding to pick-up, knock-out and evaporation processes [28]:

$$\frac{{\rm d}\sigma}{{\rm d}\varepsilon_\alpha} = \frac{{\rm d}\sigma^{\text{pick-up}}}{{\rm d}\varepsilon_\alpha} + \frac{{\rm d}\sigma^{\text{knock-out}}}{{\rm d}\varepsilon_\alpha} + \frac{{\rm d}\sigma^{\text{evap}}}{{\rm d}\varepsilon_\alpha}. \tag{15}$$

To describe a pick-up reaction, the Iwamoto-Harada model is used [23]. The differential cross-section (energy spectrum) of pre-equilibrium emission in the frame of the hybrid exciton model is written as

$$\frac{{\rm d}\sigma^{\text{pick-up}}}{{\rm d}\varepsilon_\alpha} = \sigma_{\rm non} \sum_{n=n_0} \sum_{l+m=4} F_{lm} \frac{\omega(p-l, h, E - Q_\alpha - \varepsilon_\alpha)}{\omega(p,h,E)} \cdot \frac{\lambda_{\rm c}^\alpha(\varepsilon_\alpha)}{\lambda_{\rm c}^\alpha(\varepsilon_\alpha) + \lambda_{+}^\alpha(\varepsilon_\alpha)} g_\alpha D_n \tag{16}$$

which has the same structure as the pick-up model for deuteron emission described in the previous section, the "d" superscript being now replaced by the "α" superscript, with obvious changes in the other quantities.

In particular, the α-particle emission rate is calculated as follows:

$$\lambda_{\mathrm{c}}^{\alpha} = \frac{(2s_\alpha + 1)\mu_\alpha \varepsilon_\alpha \sigma_{\mathrm{inv}}^{\alpha}(\varepsilon_\alpha)}{\pi^2 \hbar^3 g_\alpha}, \tag{17}$$

where s_α and μ_α are spin and the reduced mass of the α-particle, $\sigma_{\mathrm{inv}}^{\alpha}$ is the inverse reaction cross-section. The intra-nuclear transition rate due to the interaction of the α-particle with nucleons is written in the form

$$\lambda_{+}^{\alpha} = \frac{2 \cdot W_{\mathrm{opt}}^{\alpha}}{\hbar}, \tag{18}$$

where $W_{\mathrm{opt}}^{\alpha}$ is the imaginary part of the α-particle optical potential. Finally, the $F_{l,m}$ formation factors obtained in ref. [23] were used to calculate $\mathrm{d}\sigma^{\text{pick-up}}/\mathrm{d}\varepsilon_\alpha$.

In the present work, the α-particle knock-out process is described in a modified version of the "prepared cluster" model [29] where the shortcomings noted in refs. [30, 31] have been removed; moreover, the present version gives a description of the high-energy part of the non-equilibrium α-spectrum close to the knock-out model [30] and is of simpler use in numerical applications.

We consider a three-component system consisting of neutrons, protons and α-particles. The state density of such a system can be described by a modified Strutinsky-Ericson formula:

$$\omega(\pi, \tilde{\pi}, \nu, \tilde{\nu}, \alpha, \tilde{\alpha}) = \frac{g_\pi^{\pi+\tilde{\pi}} g_\nu^{\nu+\tilde{\nu}} g_\alpha^{\alpha+\tilde{\alpha}}}{\pi!\nu!\alpha!\tilde{\pi}!\tilde{\nu}!\tilde{\alpha}!} \cdot \frac{E^{n-1}}{(n-1)!}, \tag{19}$$

where $\pi, \tilde{\pi}, \nu, \tilde{\nu}, \alpha, \tilde{\alpha}$ are the numbers of protons, neutrons, α-particles and of the corresponding holes in n-exciton states ($n = \pi+\tilde{\pi}+\nu+\tilde{\nu}+\alpha+\tilde{\alpha}$); g_π, g_ν, g_α are single-particle state densities for protons, neutrons, and α-particles, respectively.

The ratio of state densities for the system after α-emission and for the compound nucleus that defines the α-emission spectrum can be expressed through the ratio of densities for the one-component system. The expression of the knock-out α-particle spectrum can be written in this case as follows:

$$\frac{\mathrm{d}\sigma^{\text{knock-out}}}{\mathrm{d}\varepsilon_\alpha} = \sigma_{\mathrm{non}} \sum_{n=n_0} \varphi_\alpha \cdot \frac{g}{g_\alpha p} \cdot \frac{\omega(p-1, h, E - Q_\alpha - \varepsilon_\alpha)}{\omega(p, h, E)} g_\alpha \frac{\lambda_{\mathrm{c}}^{\alpha}(\varepsilon_\alpha)}{\lambda_{\mathrm{c}}^{\alpha}(\varepsilon_\alpha) + \lambda_{+}^{\alpha}(\varepsilon_\alpha)} \cdot D_n, \tag{20}$$

where φ_α is the probability of interaction of the incident particle with the "prepared" α-cluster [31].

At incident nucleon energies higher than 100 MeV, the non-equilibrium α-particle emission can take place after the non-equilibrium emission of a neutron, or a proton. In this case, the energy spectrum of the α-particles formed in a pick-up process and emitted

after a pre-equilibrium nucleon can be written as follows:

$$
\begin{aligned}
(21)\qquad & \frac{\mathrm{d}\sigma_2^{\text{pick-up}}}{\mathrm{d}\varepsilon_\alpha} = \\
& = \sigma_{\text{non}} \sum_{x=\pi,\nu}^{2} \sum_{n=n_0} R_x(n) \cdot \frac{\omega(p-1,h,E-Q_x-\varepsilon_x)}{\omega(p,h,E)} \cdot \frac{\lambda_{\text{c}}^x(\varepsilon_x)}{\lambda_{\text{c}}^x(\varepsilon_x)+\lambda_+^x(\varepsilon_x)} g_x D_n \times \\
& \quad \times \sum_{n'=p+h-1} \sum_{l+m=4} F_{l,m}(\varepsilon_\alpha) \frac{\omega(p'-l,h',E-Q_x-\varepsilon_x-Q_\alpha-\varepsilon_\alpha)}{\omega(p',h',E-Q_x-\varepsilon_x)} \times \\
& \quad \times \frac{\lambda_{\text{c}}^\alpha(\varepsilon_\alpha)}{\lambda_{\text{c}}^\alpha(\varepsilon_\alpha)+\lambda_+^\alpha(\varepsilon_\alpha)} g_\alpha D_{n'},
\end{aligned}
$$

where x is a neutron/proton index, Q_x is the binding energy of particle x in a compound nucleus, $R_x(n)$ is the factor describing the number of protons and neutrons in the n-exciton state, Q_α is the separation energy of the α-particle in the nucleus after emission of particle x.

An analogous formula can be written for the component corresponding to the α-particle knock-out process that occurs after pre-equilibrium nucleon emission. It involves a pre-formation factor, φ_α:

$$
\begin{aligned}
(22)\qquad & \frac{\mathrm{d}\sigma_2^{\text{knock-out}}}{\mathrm{d}\varepsilon_\alpha} = \\
& = \sigma_{\text{non}} \sum_{x=\pi,\nu}^{2} \sum_{n=n_0} R_x(n) \cdot \frac{\omega(p-1,h,E-Q_x-\varepsilon_x)}{\omega(p,h,E)} \cdot \frac{\lambda_{\text{c}}^x(\varepsilon_x)}{\lambda_{\text{c}}^x(\varepsilon_x)+\lambda_+^x(\varepsilon_x)} g_x D_n \times \\
& \quad \times \sum_{n'=p+h-1} \varphi_\alpha \frac{g}{g_\alpha p'} \frac{\omega(p'-1,h',E-Q_x-\varepsilon_x-Q_\alpha-\varepsilon_\alpha)}{\omega(p',h',E-Q_x-\varepsilon_x)} \times \\
& \quad \times \frac{\lambda_{\text{c}}^\alpha(\varepsilon_\alpha)}{\lambda_{\text{c}}^\alpha(\varepsilon_\alpha)+\lambda_+^\alpha(\varepsilon_\alpha)} g_\alpha D_{n'}.
\end{aligned}
$$

Parameters of the model are the sum of the probabilities of α-particle formation, $\Sigma F_{l,m}$, with $l+m=4$, and the interaction probability of the incident nucleon with the "prepared" α-particle, φ_α. Moreover, uncertainties exist in the single-particle state density, g_α, and the imaginary part of the optical potential, W_{opt}^α, for α-particles. The values of $\Sigma F_{l,m}$ and φ_α in formulas (21) and (22) can be determined independently. At an incident energy of 90 MeV, the high-energy part of experimental α-spectra [32] is essentially reproduced by the knock-out model, while the pick-up component, $\mathrm{d}\sigma^{\text{pick-up}}/\mathrm{d}\varepsilon_\alpha$, is responsible for the soft part of the non-equilibrium spectrum. For this reason, $\Sigma F_{l,m}$ and φ_α can be obtained from the comparison between calculated and experimental spectra, if the values of g_α and the imaginary part of the optical potential W_{opt}^α are known.

Various theoretical estimations exist for g_α: $g_\alpha = g/4.0$ [29], $g_\alpha = g/8.0$ [31], $g_\alpha = A/10.36$ [33] and $g_\alpha = 4g$ [34], where g is the single-particle state density for nucleons. The uncertainty in g_α, however, is not very important for the calculation of α-spectra, as far as the variation of g_α is equivalent to re-defining other parameters, for example W_{opt}^α. In the present work g_α was chosen equal to g. The energy dependence of W_{opt}^α was determined by comparison of theoretical and experimental α-particle spectra for proton-induced reactions at energies between 18 and 90 MeV [32, 35-39]. Use was also made of

the cross-sections of (n, α) reactions obtained from the analysis of various experiments at $E_{\mathrm{n}} = 14.5\,\mathrm{MeV}$ [40] for 42 nuclei with nuclear charge $Z > 60$.

The following values of parameters were used in the calculations: $\Sigma F_{l,m} = 0.3$, and $\varphi_\alpha = 0.012$. The single-particle state density for α-particles was set to $g_\alpha = A/13$. The imaginary part of the optical potential was calculated as follows: $W^\alpha_{\mathrm{opt}} = \varepsilon_\alpha \cdot W'/\varepsilon_0$ at $\varepsilon_\alpha < \varepsilon_0$ and $W^\alpha_{\mathrm{opt}} = W'$ at $\varepsilon_\alpha > \varepsilon_0$, where ε_α is the α-particle energy, $W' = \beta W_0$, W_0 being the value of the imaginary part of the optical potential in the centre of the nucleus, $\varepsilon_0 = 0.228A$ and $\beta = 0.25$. The value of W_0 was taken to be

$$W_0 = 10.0 + 0.345(A - 2Z)\,\mathrm{MeV}. \tag{23}$$

4. – Comparisons and discussion

In figs. 1–12 we compare the results of calculations carried out with the HMS-ALICE and ALICE-IPPE codes with available experimental data on excitation functions for proton-induced reactions on nuclei in a mass region from Mn-55 to Bi-209 and in the energy interval from the reaction thresholds up to 200 MeV [41-57]. On each figure, the points are experimental data, the solid line is the result of the ALICE-IPPE calculations with the generalized superfluid model for level densities according to subsect. **3**˙2; the dashed line corresponds to ALICE-IPPE with Fermi-gas level densities including pairing corrections; the dot-dashed line is the HMS-ALICE calculation with level densities of Kataria and Ramamurthy [58]; the double dot-dashed line is again HMS-ALICE with Fermi-gas level densities. Figures 1–5 show the excitation functions for relatively "simple" reactions, $^{56}\mathrm{Fe}(p, 2pn)$, $^{209}\mathrm{Bi}(p, 3n)$, $^{88}\mathrm{Sr}(p, 4n)$, $^{127}\mathrm{I}(p, 5n)$, and $^{89}\mathrm{Y}(p, p5n)$ with emission of several nucleons. One can see that different calculations are in reasonable mutual agreement for the reactions with emission of neutrons, $^{209}\mathrm{Bi}(p, 3n)$, $^{88}\mathrm{Sr}(p, 4n)$ and $^{127}\mathrm{I}(p, 5n)$, and give a good description of experimental data near the threshold region. The differences become more pronounced for the reactions where also protons are emitted, $^{56}\mathrm{Fe}(p, 2pn)$ and $^{89}\mathrm{Y}(p, p5n)$. In general, the differences in the calculated cross-sections increase with increasing number of emitted particles.

The reactions with the emission of light charged particles (alpha-particles, in particular) deserve special consideration. Figure 6 shows the experimental excitation function for the $^{90}\mathrm{Zr}(p, 2n2p)$ reaction, whose structure, including a local maximum followed by a shoulder at higher energy, is due to the contribution of two processes, the emission of an alpha-particle and the emission of four uncorrelated nucleons (two protons and two neutrons). The thresholds of these processes differ by the binding energy of the α-particle (28.2 MeV). The main contribution to the low-energy part of the excitation function around the first local maximum is due to the evaporation of α-particles from an equilibrated system. In this energy region, the results of calculations using different approaches are not drastically different because the evaporation mechanism parameters are similar in the two codes.

It is well known, however, that the region above the local maximum is determined by pre-equilibrium processes. Thus, in this region, the differences in the description of the emission mechanisms of α-particles can be investigated more thoroughly. The result of calculations with different codes show large discrepancies, up to three orders of magnitude in the energy region of 30–40 MeV for the $^{90}\mathrm{Zr}(p, 2n2p)$ reaction. It was noted in ref. [12] that some deficiencies in the HMS-ALICE results for the excitation functions around 50–80 MeV could be due to the absence of a direct (p, α) knock-out mechanism.

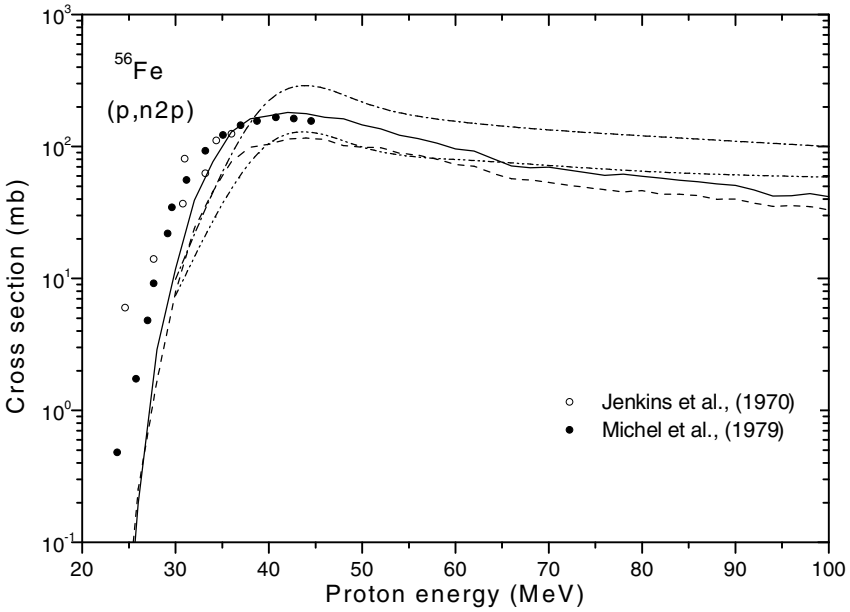

Fig. 1. – Excitation function for the $^{56}\mathrm{Fe}(p, n2p)$ reaction calculated using different approaches (curves) in comparison with experimental data (points). Solid line: ALICE-IPPE calculation with the generalized superfluid model for level density; dashed line: ALICE-IPPE with Fermi-gas level density including pairing corrections; dot-dashed line: HMS-ALICE with the level density of Kataria and Ramamurthy [58]; double-dot-dashed line: HMS-ALICE with Fermi-gas level density.

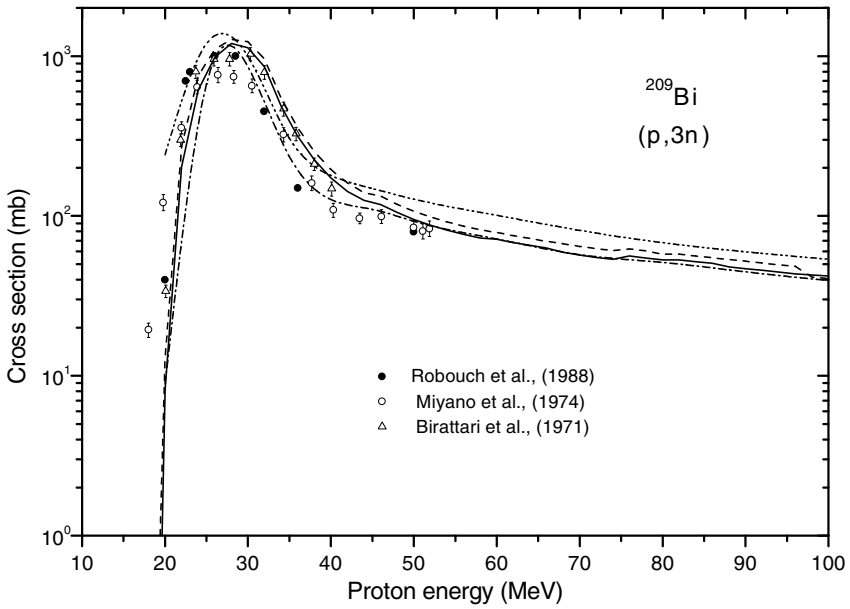

Fig. 2. – As in fig. 1, but for the $^{209}\mathrm{Bi}(p, 3n)$ reaction.

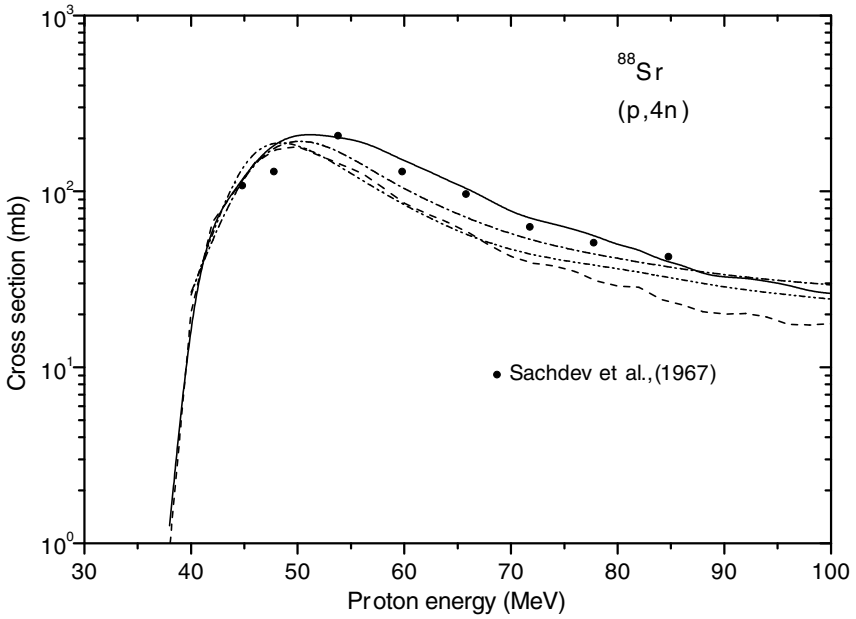

Fig. 3. – As in fig. 1, but for the $^{88}\mathrm{Sr}(p, 4n)$ reaction.

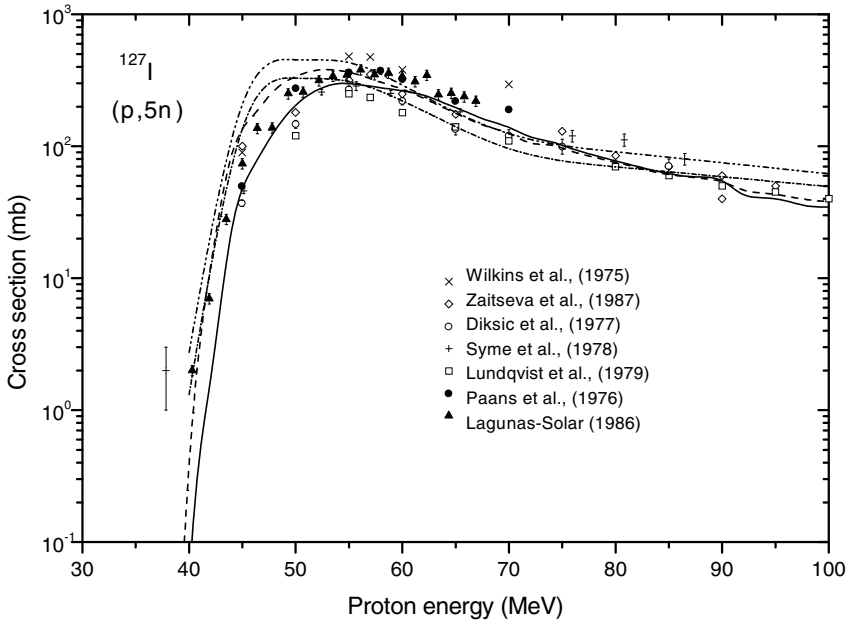

Fig. 4. – As in fig. 1, but for the $^{127}\mathrm{I}(p, 5n)$ reaction.

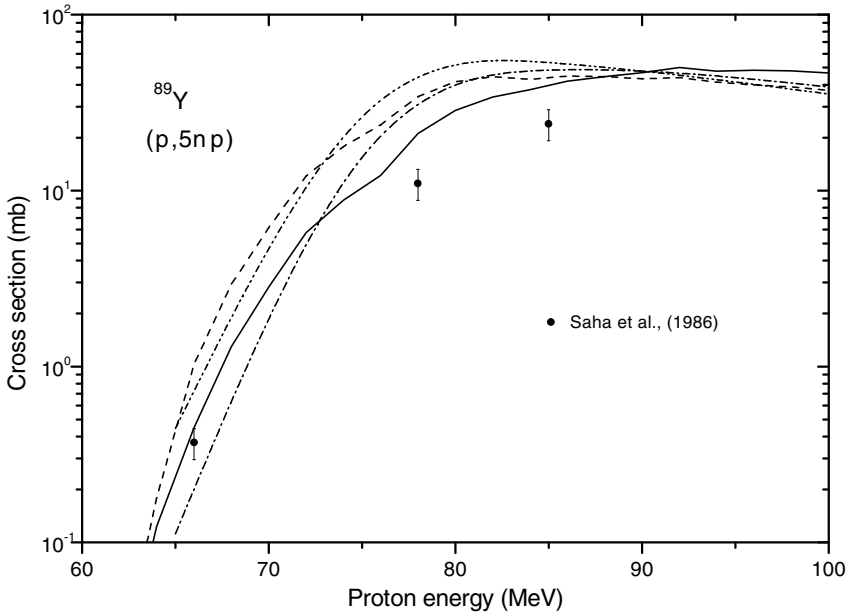

Fig. 5. – As in fig. 1, but for the $^{89}\mathrm{Y}(p, 5np)$ reaction.

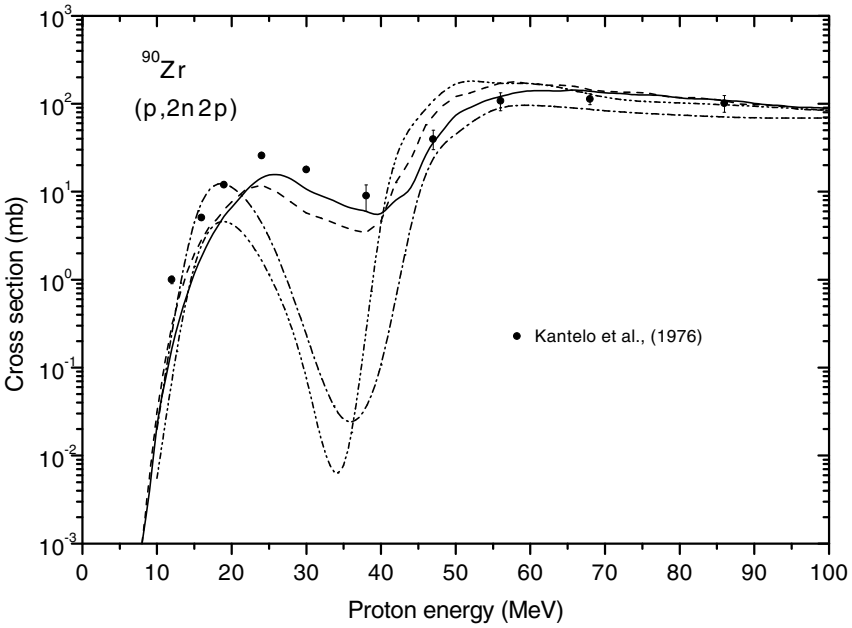

Fig. 6. – As in fig. 1, but for the $^{90}\mathrm{Zr}(p, 2n2p)$ reaction.

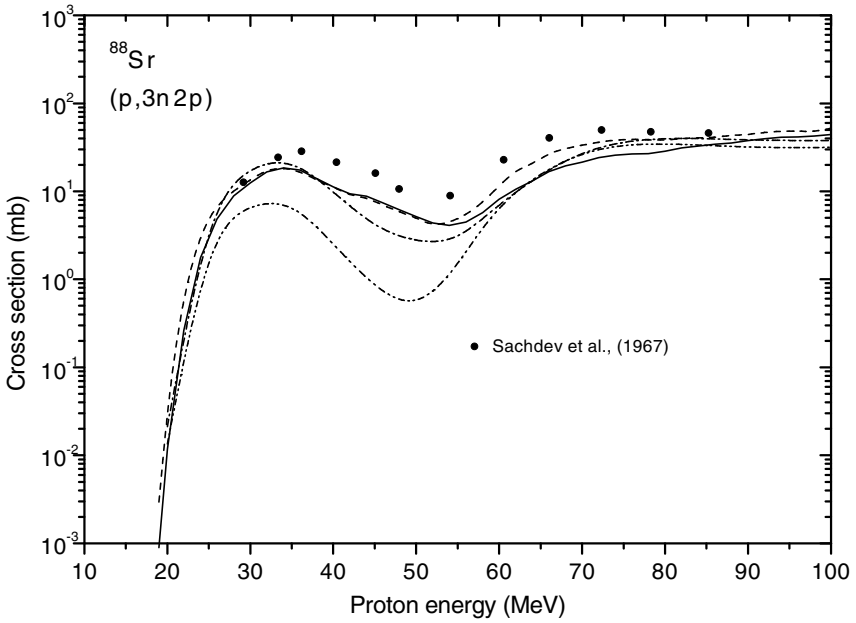

Fig. 7. – As in fig. 1, but for the $^{88}\mathrm{Sr}(p, 3n2p)$ reaction.

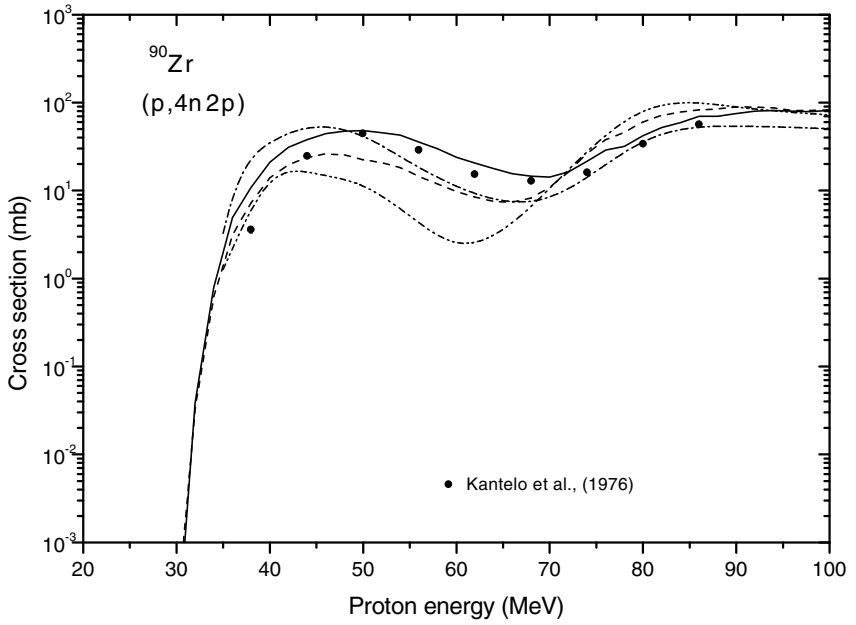

Fig. 8. – As in fig. 1, but for the $^{90}\mathrm{Zr}(p, 4n2p)$ reaction.

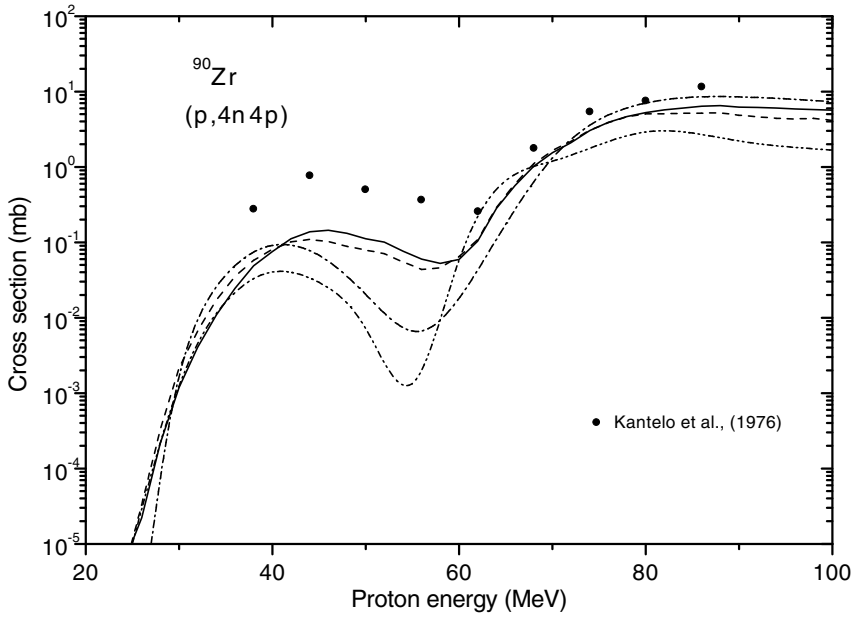

Fig. 9. – As in fig. 1, but for the $^{90}\mathrm{Zr}(p, 4n4p)$ reaction.

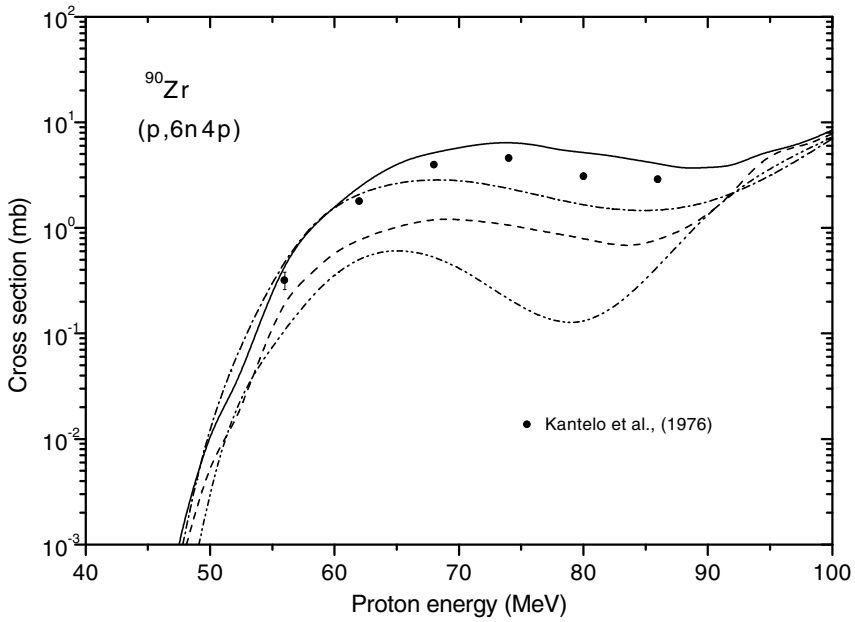

Fig. 10. – As in fig. 1, but for the $^{90}\mathrm{Zr}(p, 6n4p)$ reaction.

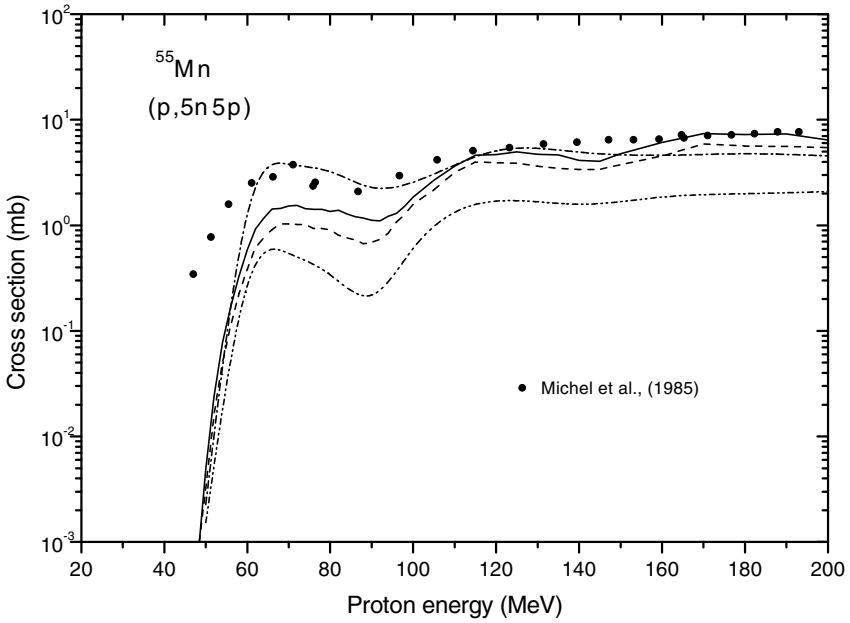

Fig. 11. – As in fig. 1, but for the $^{55}\mathrm{Mn}(p, 5n5p)$ reaction.

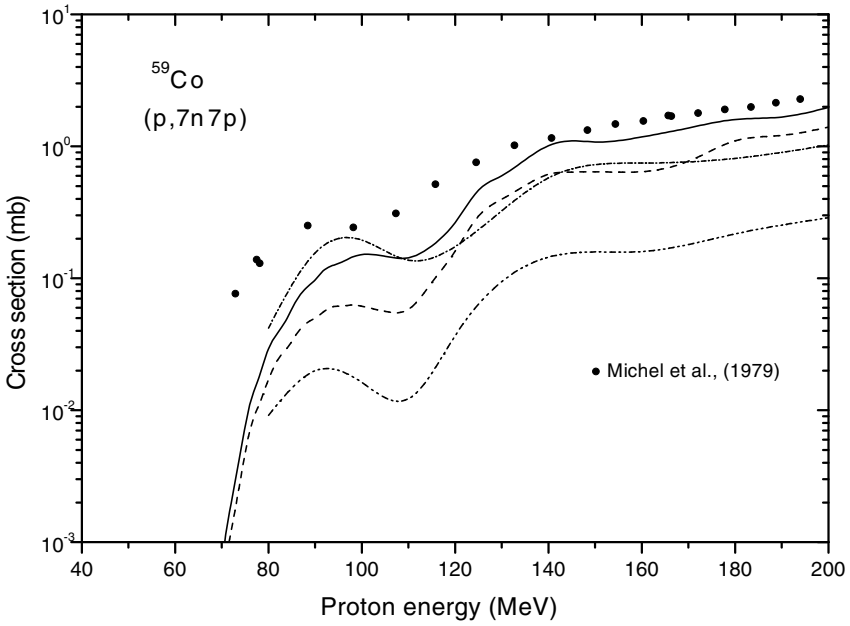

Fig. 12. – As in fig. 1, but for the $^{59}\mathrm{Co}(p, 7n7p)$ reaction.

One can see in fig. 6 that the HMS-ALICE calculations strongly underestimate the experimental excitation function for both models used for level densities. The most probable explanation is that the emission of α-particles is due to several competing mechanisms. In this energy region, both knock-out and pick-up mechanisms are important. In the ALICE-IPPE code these processes are all taken into account, hence the better description of experimental data in comparison with HMS-ALICE. The effect of the level density formalism is not so important in this case. The differences of results of these codes can give information on the competition of various mechanisms for the emission of α-particles in this energy region.

When the number of emitted particles increases, as in the $^{88}\mathrm{Sr}(p, 3n2p)$ reaction shown in fig. 7, the effect is not so pronounced as in the $^{90}\mathrm{Zr}(p, 2n2p)$ reaction, but, nevertheless, the importance of taking into account all the mechanisms of pre-equilibrium emission of α-particles is still evident. Figures 8–10 show the excitation functions for the reactions $^{90}\mathrm{Zr}(p, 4n2p)$, $^{90}\mathrm{Zr}(p, 4n4p)$ and $^{90}\mathrm{Zr}(p, 6n4p)$ induced on the same target nucleus, $^{90}\mathrm{Zr}$. There are considerable differences in the calculations, due both to level density models and to the non-equilibrium α-particle emission mechanisms. For the reactions with the emission of two α-particles and a larger number of emitted particles (figs. 9 and 10), the energy region where the calculations show sizable differences is even larger. For the $^{55}\mathrm{Mn}(p, 5n5p)$ and $^{59}\mathrm{Co}(p, 7n7p)$ reactions, where a large number of particles are emitted, the leading effect is due to level density models. One can conclude that the generalized superfluid model for level density gives in general better results than the other approaches.

The reactions leading to the emission of light charged particles are particularly relevant to the development of concepts of hybrid accelerator-driven power systems. Some important properties of the target, which is an essential constituent of the system, such as gas production, radiation resistance in a high-energy proton and neutron fluxes and, finally, the safety and life-time of the system will be determined to a large degree by these types of nuclear reactions. Therefore, taking into account all possible reaction mechanisms for a reliable estimation of these microscopic cross-sections is also important for a detailed design of accelerator-driven systems.

* * *

The authors are very grateful to Prof. M. Blann for his help in the use of HMS-ALICE and to Prof. A. V. Ignatyuk for useful discussions and valuable comments.

REFERENCES

[1] Koning A. J., report NEA/NSC/DOC(93)6-ECN-C–93-005 (1993); Shubin Yu. N., in *Nuclear Methods for Transmutation of Nuclear Waste, Dubna, 29-31 May 1996*, (World Scientific) 1997, p. 135.

[2] Koning A. J., in *Proceedings of the Second International Conference on Accelerator-Driven Transmutation Technologies and Applications, Kalmar, 3-7 June 1996*, edited by H. Condé, Vol. **1** (Uppsala University Press) 1997, p. 438.

[3] Bertini H. W., *Phys. Rev.*, **188** (1969) 1711.

[4] Barashenkov V. S., Toneev V. D. and Chigrinov C. A., *At. Energy*, **34** (1974) 480.

[5] HETC. Code Package CCC-178, ORNL-4744., Radiation Shielding Information Center, Oak Ridge National Laboratory.

[6] Filges D. *et al.*, report JUL-1960, KFA Jülich, Germany (1984).

[7] Hofmann P., Iljinov A. S., Kim Y. S., Mebel M. V., Daniel H., David P., von Egidy T., Haninger T., Hartmann F. J., Jastrzebski J., Kurcewicz W., Lieb J., Machner H., Plendl H. S., Riepe G., Wright B. and Ziock K., *Phys. Rev. C*, **49** (1994) 2555.
[8] Iljinov A. S., Mebel M. V., Bianchi N., De Sanctis E., Guaraldo C., Lucherini V., Muccifora V., Polli E., Reolon A. R. and Rossi P., *Nucl. Phys. A*, **543** (1992) 517; Iljinov A. S., Mebel M. V., Guaraldo C., Lucherini V., De Sanctis E., Bianchi N., Levi Sandri P., Muccifora V., Poli E., Reolon A. R., Rossi P. and Lo Nigro S., *Phys. Rev. C*, **39** (1989) 1420.
[9] Blann M., *Phys. Rev. C*, **54** (1996) 1341.
[10] Blann M., in *Workshop on Computation and Analysis of Nuclear Data Relevant to Nuclear Energy and Safety, Trieste, 10 February-13 March 1992*, edited by M. K. Mehta and J. J. Schmidt (World Scientific, London) 1993.
[11] Dityuk A. I., Konobeyev A. Yu., Lunev V. P. and Shubin Yu. N., report INDC(CCP)-410, IAEA, Vienna (1998).
[12] Mebel M. V., Iljinov A. S., Grandi C., Reffo G. and Blann M., *Nucl. Instrum. Methods Phys. Res. A*, **398** (1997) 324.
[13] Ignatyuk A. V., *Statistical properties of excited atomic nuclei* (Energoatomizdat, Moscow) 1983 (in Russian).
[14] Ignatyuk A. V., *Yader. Fiz.*, **21** (1975) 20.
[15] Blokhin A. I., Ignatyuk A. V., Pashchenko A. B., Sokolov Yu. V. and Shubin Yu. N., *Commun. Acad. Sci. USSR*, **49** (1985) 962.
[16] Blokhin A. I., Ignatyuk A. V. and Shubin Yu. N., *Sov. J. Nucl. Phys.*, **48** (1988) 232.
[17] Ignatyuk A. V., Weil J. L., Raman S. and Kahane S., *Phys. Rev. C*, **47** (1993) 1504.
[18] Ignatyuk A. V., Istekov K. K. and Smirenkin G. N., *Yad. Fiz.*, **29** (1979) 875.
[19] Ignatyuk A. V., Stavinsky V. S. and Shubin Yu. N., in *Nuclear Data for Reactors*, **2** (1970) p. 885.
[20] Myers W. D., *Droplet Model of Atomic Nuclei* (IFI/Plenum Press, New York) 1977.
[21] Myers W. D. and Swiatecki W. J., *Arkiv Fys.*, **36** (1967) 343.
[22] Hansen G. and Jensen A. S., *Nucl. Phys. A*, **406** (1983) 236.
[23] Iwamoto A. and Harada K., *Phys. Rev. C*, **26** (1982) 1821.
[24] Sato N., Iwamoto A. and Harada K., *Phys. Rev. C*, **28** (1983) 1527.
[25] Gadioli E., report INFN/BE-88-2, Milano, Italy (1988).
[26] Dobes J. and Betak E., in *Proceedings of the International Conference on Reaction Models 77, Balatonfüred* 1977, p. 195.
[27] Kalbach C., *Z. Phys. A*, **283** (1977) 401.
[28] Konobeyev A. Yu., Lunev V. P. and Shubin Yu. N., report IPPE-2465, Obninsk, Russia (1995).
[29] Milazzo-Colli L. and Braga-Marcazzan G. M., *Nucl. Phys. A*, **210** (1973) 297.
[30] Ferrero A., Gadioli E., Gadioli Erba E., Iori I., Molho N. and Zetta L., *Z. Phys. A*, **293** (1979) 123.
[31] Oblozinsky P. and Ribansky I., *Phys. Lett. B*, **74** (1978) 6.
[32] Wu J. R., Chang C. C. and Holmgren H. D., *Phys. Rev. C*, **19** (1979) 698.
[33] Gadioli E. and Gadioli Erba E., *Z. Phys. A*, **299** (1981) 1.
[34] Kadmensky S. G. and Furman V. I., *Alpha-decay and nuclear reactions* (Moscow, Energoatomizdat) 1985 (in Russian).
[35] Lewandowski Z., Loeffler E., Wagner R., Mueller H. H., Reichart W., Schober P., Gadioli E. and Gadioli Erba E., *Lett. Nuovo Cimento*, **28** (1980) 15.
[36] Kumabe I., Inenaga Y., Hyakutake M., Koori N., Watanabe Y., Ogawa K. and Orito K., *Phys. Rev. C*, **38** (1988) 2531.
[37] Ferrero A., Iori I., Molho N. and Zetta L., report INFN/BE-78/6, Milano, Italy (1978).
[38] Bertrand F. E. and Peelle R. W., *Phys. Rev. C*, **8** (1973) 1045.
[39] Chevarier A., Chevarier N., Demeyer A., Hollinger G., Pertosa P. and Tran Minh Duc, *Phys. Rev. C*, **11** (1975) 886.

[40] Konobeyev A. Yu., Lunev V. P. and Shubin Yu. N., *Nucl. Instrum. Methods Phys. Res. B*, **108** (1996) 233.
[41] Michel R., Peiffer F. and Stuck R., *Nucl. Phys. A*, **441** (1985) 617.
[42] Jenkins I. L. and Wain I. L., *J. Inorg. Nucl. Chem.*, **32** (1970) 1419.
[43] Michel R., Brinkmann G., Weigel H. and Herr W., *Nucl. Phys. A*, **322** (1979) 40.
[44] Sachdev D. R., Porile N. T. and Yaffe L., *Can. J. Chem.*, **45** (1967) 1149.
[45] Saha G. B., Porile N. T. and Yaffe L., *Phys. Rev.*, **144** (1966) 962.
[46] Kantelo M. V. and Hogan M. V., *Phys. Rev. C*, **14** (1976) 64.
[47] Wilkins S. R., Shimose S. T., Hines H. H. *et al.*, *Int. J. Appl. Rad. Isotopes*, **26** (1975) 279.
[48] Paans A. M., Vaalburg W., van Herk G. and Woldring M. G., *Int. J. Appl. Rad. Isotopes*, **27** (1976) 465.
[49] Diksic M. and Yaffe L., *J. Inorg. Nucl. Chem.*, **39** (1977) 1299.
[50] Syme D. B., Wood E., Blair I. M., Kew S., Perry M. and Cooper P., *Int. J. Appl. Rad. Isotopes*, **29** (1978) 29.
[51] Lundqvist H., Malmborg P., Langstrom B. and Chiengmai S. N., *Int. J. Appl. Rad. Isotopes*, **30** (1979) 39.
[52] Lagunas-Solar M. C., Carvacho O. F., Bo-Li Liu, Jin Y. and Sun Zh. X., *Int. J. Appl. Rad. Isotopes*, **37** (1986) 823.
[53] Zaitseva N. G., Knotek O., Kim Sen Khan and Mikec P., *Radiokhimiya*, **3** (1987) 391.
[54] Kantelo M. V. and Hogan J. J., *Phys. Rev. C*, **13** (1976) 1095.
[55] Robouch B. V. and Gentilini A., ENEA report RT/FUS/87/31, Frascati, Italy (1988).
[56] Miyano K., Sekikawa M., Kaneko T. and Nomoto M., *Nucl. Phys. A*, **230** (1974) 98.
[57] Birattari C., Gadioli E., Grassi Strini A. M., Strini G., Tagliaferri G. and Zetta L., *Nucl. Phys. A*, **166** (1971) 605.
[58] Kataria S. K. and Ramamurthy V. S., *Nucl. Phys. A*, **349** (1980) 10; Kataria S. K., Ramamurthy V. S., Blann M. and Komoto T. T., *Nucl. Instrum. Methods Phys. Res. A*, **288** (1980) 585.